# Fully Automated Spleen Localization and Segmentation Using Machine Learning and 3D Active Contours

Alexander Wood<sup>1,2</sup>, S.M.Reza Soroushmehr<sup>1,2</sup>, Negar Farzaneh<sup>1</sup>, David Fessell<sup>3</sup>, Kevin R. Ward<sup>2,4</sup>, Jonathan Gryak<sup>1</sup>, Delaram Kahrobaei<sup>5</sup>, Kayvan Najarian<sup>1,2,4</sup>

Abstract—Automated segmentation of the spleen in CT volumes is difficult due to variations in size, shape, and position of the spleen within the abdominal cavity as well as similarity of intensity values among organs in the abdominal cavity. In this paper we present a method for automated localization and segmentation of the spleen within axial abdominal CT volumes using trained classification models, active contours, anatomical information, and adaptive features. The results show an average Dice score of 0.873 on patients experiencing various chest, abdominal, and pelvic traumas taken at different contrast phases.

Keywords - Image segmentation, organ localization, machine learning

#### I. Introduction

Automated spleen segmentation can be used as preprocessing for fast diagnosis of the severity of blunt splenic injury, one of the most commonly injured abdominal organs. Computed tomography (CT) scanning is the modality of choice when gauging abdominal trauma [1]. The severity of blunt splenic injury is often a criterion for determining the necessity of surgical intervention [2].

In addition to blunt injury detection, changes in splenic volume can assist in long-term monitoring of a range underlying conditions such as infection, immunological disorders, circulatory disorders, leukemia, and haematopoietic diseases [3]. The gold standard method for estimation of in vivo splenic volume is via summation of splenic volume in contiguous axial CT scans. However, manual segmentation is time-consuming and subject to variations based on the observer [4].

While scans captured at the portal venous phase, approximately 80 seconds after injection of contrast dye, are preferred for visualization of the spleen in CT scans, prior knowledge of contrast phase cannot always be assumed [1]. Therefore, any computer-aided diagnosis system (CAD) must be robust to variations in contrast phase. Two major

<sup>1</sup> Department of Computational Medicine and Bioinformatics, University

challenges a CAD must address are localization of an organ within a CT volume and segmentation of its boundaries in each scan [5]. Previous methods used to localize the spleen include ensemble learning approaches [6] as well as localization during multi-organ segmentation using relative location [5], [7], [8], [9], [10], [11]. Much of previous work in spleen segmentation utilized atlas-based methods [12], [13], [7], [8], [9]. However, a previously derived atlas may not be robust to the variations in the size and shape of injured spleens [14]. Other past approaches include neural networks [5], multi-boost learning [10], fast marching methods [11].

We propose an algorithm for fully automated localization and segmentation of the spleen within an axial CT volume. Localization utilizes machine learning techniques to identify a small region contained within the spleen. No prior knowledge regarding which portions of the chest, abdomen, and/or pelvic region are included in the CT volume are required. Segmentation is performed via series of reinitialized active contours using this small region as an seed mask. Relative pixel intensity within the mask is observed before each re-initialization to refine the contour and avoid over-segmentation. Results show that the proposed method performs well in the presence blunt abdominal trauma.

### II. METHODS

The proposed algorithm incorporates a variety of information, including active contours, texture information, and spatial information. The broad flow of the algorithm is illustrated in Figure 1. First, we apply preprocessing to the raw images. Next, spatial and anatomical information is used to localize the spleen. Localization occurs on two planes. The abdomen is localized along the axis of the body. The abdominal region is then used to run a targeted detection algorithm which selects a single image in the CT volume which contains the spleen. An initial spleen location is then determined using the relative position of the spleen within the abdomen with respect to the spine, ribcage, and relative pixel intensity information. We then apply an adaptive bright object mask and move on to perform segmentation.

### A. Preprocessing

Preprocessing is applied to the images in order to remove noise and artifacts outside the abdomen. Preprocessing consists of standard contrast adjustment based on metadata provided in the dicom volumes followed by the abdomen

of Michigan, Ann Arbor, MI, USA

<sup>2</sup> Michigan Center for Integrative Research in Critical Care University of Michigan, Ann Arbor, MI, USA

<sup>&</sup>lt;sup>3</sup> Department of Radiology, University of Michigan, Ann Arbor, MI, USA

<sup>&</sup>lt;sup>4</sup> Department of Emergency Medicine, University of Michigan, Ann Arbor, MI, USA

<sup>&</sup>lt;sup>5</sup> Department of Computer Science, The Graduate Center, CUNY, New York, New York, USA

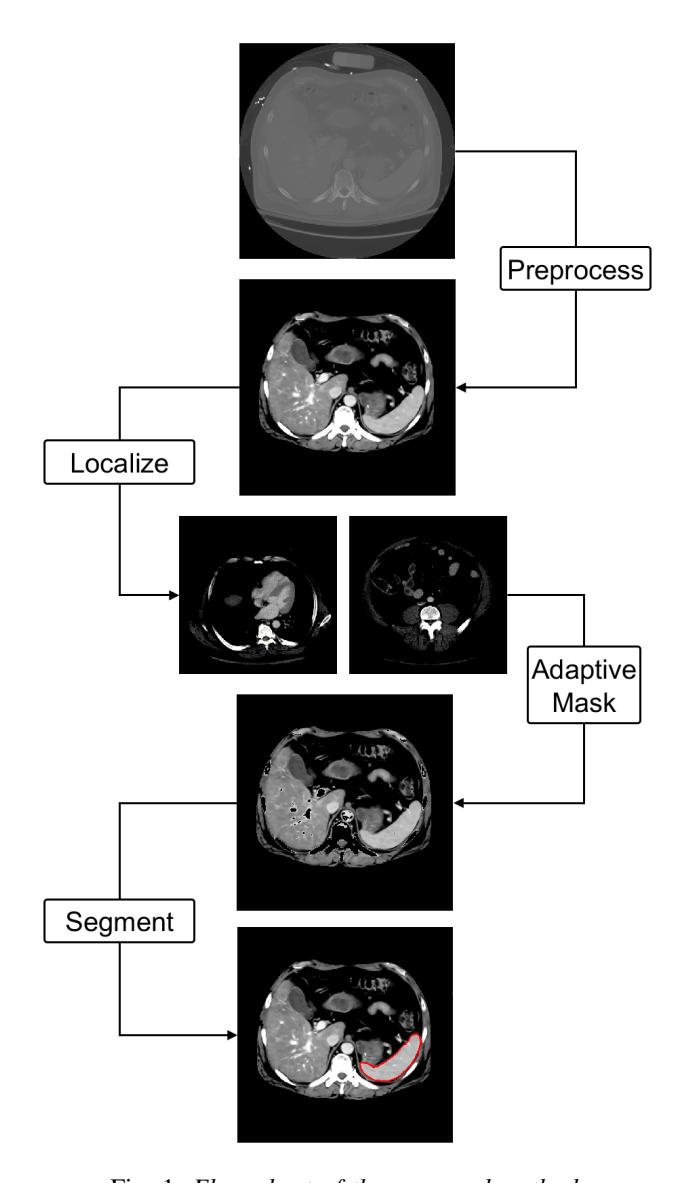


Fig. 1: Flow chart of the proposed method.

masking procedure of Soureshmehr et. al. to remove artifacts outside of the abdomen [14]. In order to further emphasize abdominal organs within the region, the dimmest 30% of possible pixel intensities are removed and the image is normalized via intensity stretching. The non-local means filter (NLMF) is applied to perform image denoising, and local contrast enhancement is performed to sharpen edges. Figure 1 shows the raw input image and the result post-preprocessing.

#### B. Vertical localization

We begin by localization of the abdominal cavity in order to narrow down a region of interest. We define the abdominal cavity as beginning at the first CT image containing the liver and ending at the first CT image containing the iliac crest. Figure 1 provides an example of slices selected as the top and bottom of the abdominal cavity. All object detectors are boosted cascading object detectors, trained to

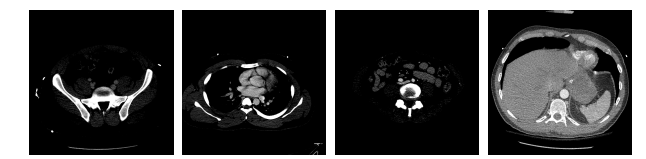


Fig. 2: Positive regions targeted by the four detectors. From left to right, they target the portion of the pelvis containing the iliac crest, the portion of the heart where the ventricles are visible and the liver is not visible, the portion of the abdomen below the kidneys and above the pelvis, and slices containing the spleen but not the heart or both kidneys.

detect recognizable regions within the abdomen using Haar-like features [15].

Pelvic detection: We begin by detecting the pelvic region containing the iliac wing. In order to remove false positives, run a detector trained to localize the region of the abdomen below the kidneys and above the pelvis on all images between the first and last slices flagged by the pelvis detector. Remove images within and above this portion of the abdomen from the list of detected pelvic images.

Spine localization: Next, we need to localize the spine; it will help locate the iliac crest(s) in the next step. Locate the spine via weighted voting over imbinarizations of a collection of scans from the 10 cm region directly above the highest detected pelvis slice, which are known to contain the spinal column. To imbinarize, remove the lowest 50% of possible pixel values then apply Otsu's method to the normalized image to determine a threshold.

Iliac crest detection: The top of the pelvis is localized by moving up through the volume, beginning at the highest detected pelvic scan, and comparing each scan to the scan above it. Imbinarize the images using the above method and remove the vertebral region from both images, as well as other artifacts occurring outside of the region which should contain the ilium. Track the pelvic bones by moving up through the volume and comparing consecutive scans until the iliac bones are no longer visible.

Heart detection: Next, run a detector to locate scans containing the heart ventricles and no portion of the liver. Only run the detector on images which occur above the pelvis as detected in the previous steps.

Spleen detection: Run a targeted detection algorithm on the images within the abdominal cavity as determined above in order to localize scans which contain the spleen, are below the heart, and contain no more than one kidney. If more than one slice is detected, select the slice in the center of all detected scans.

### C. Axial localization

We localize the spleen within this axial scan via location and intensity using a method similar to [14]. Narrow down the region of interest to bottom right quarter of the abdomen in the axial scan. Next, mask the brightest 80% of possible pixel intensities in order to remove bone from the image and locate the weighted centroid of the remaining region. This

location is used to define the center of a smaller sub-region and the weighted centroid of this sub-region is located; repeat this process using a progressively smaller sub-region until it is only a few pixels in size. This small region constitutes the initial spleen localization.

# D. Adaptive mask

Next, we mask bright objects in the volume. The threshold is determined based off of the pixel intensity values of the localized spleen region. Remove the brightest pixel intensity value within the axial slice containing the detected spleen pixels as well as all pixel values outside of the spleen region. Create a histogram with 50 bins from the resulting image. Remove all values from the first and last bins, and remove all values from bins which are less than 20% as full as the maximum bin count. Divide the index of the largest remaining non-empty bin by 50 to determine your threshold percentage; for each image, remove all pixels which lie above this threshold percentage.

### E. Transition to 3D

Set up the volume of 2-D CT images as a single 3-D volume in preparation for 3D active contour segmentation. Create two volumes, the masked volume and the 3-D seed region volume. The 3D volumes are constructed "to scale," meaning each slice is repeated in the volume until the amount of space represented by a single voxel in the z-axis corresponds as closely as possible to the space represented by the width and height of a pixel in the axial plane.

# F. Automated segmentation

Use the 3-D Chan-Vese active contour algorithm for segmentation with the initial mask volume as an input mask [16]. Re-initialize the contour at regular intervals to prevent over-segmentation, using the output mask from the previous step as the input mask to initialize the next step. Start with a contraction bias heavily weighted towards expansion in order to rapidly grow the initial seed and slowly taper down this contraction bias. Let S denote the set of all pixel intensity values (with repetition) which lie within the detected spleen region after each iteration of the active contour. Let  $\hat{S}$  denote the mean of S. After each re-initialization, perform an intensity analysis to remove pixels from the mask whose intensity lies outside the range  $(\hat{S}-t,\hat{S}+t)$  for threshold value

$$t = \max\left\{\frac{\hat{S} - \min(S)}{2}, \frac{\max(S) - \hat{S}}{2}\right\}.$$

Enforce the constraint that the segmentation must encompass one three-dimensional connected component.

### III. EXPERIMENTS AND RESULTS

### A. Dataset

The University of Michigan provided CT scans for 137 patients who experienced traumatic injuries. Additional training data was obtained from the CIREN dataset containing

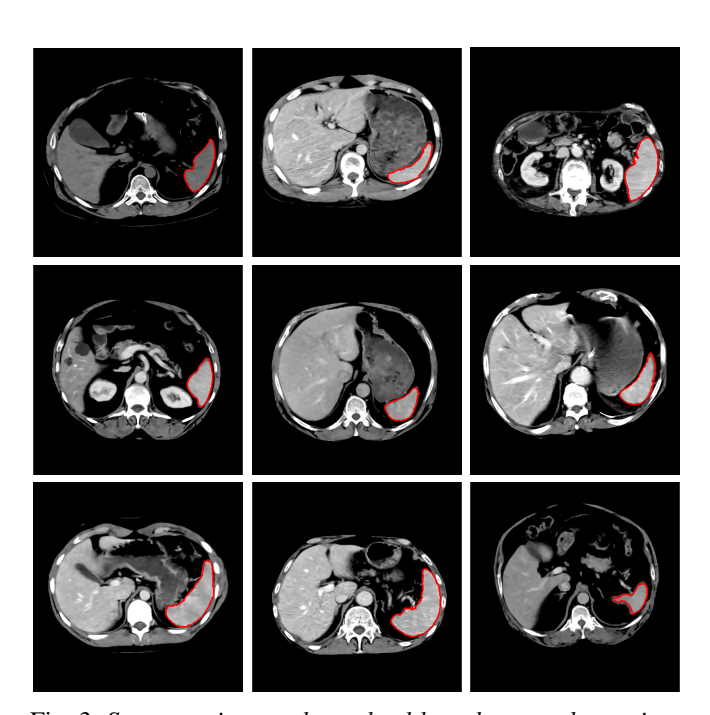


Fig. 3: Segmentation results on healthy spleens under various contrast phases.

CT volumes for patients who experienced traumatic injuries in a motor vehicle accident. For each patient we obtained an axial abdominopelvic CT volume of between 42 and 122 scans of 5mm thickness acquired and various unknown contrast phases. Manual spleen annotations reviewed by an expert radiologist were obtained for a total of 39 patients experiencing abdominal, chest, or pelvic blunt trauma.

## B. Experiments

Four boosted cascading object detectors were trained with Haar-like features over contrast-adjusted images from 108 different chest-abdomen-pelvic CT volumes in the University of Michigan and CIREN datasets [15]. Images from the testing set were not used for training. The first detector was trained to localize the middle of the heart within 1 cm of the top of the liver using 6 cascading stages using 5,515 negative samples and 137 positive samples. The second detector was trained with 356 positive samples consisting of pelvic scans and 26,636 negative samples in 20 stages. The third detector was trained using 252 positive samples consisting of slices of the abdomen from above the pelvis but below the kidneys and 3,242 negative samples, and was used to remove false positives flagged by the second detector. The last detector was trained over 205 positive samples containing the spleen and 8, 382 negative samples in 13 cascading stages. Samples in the second and third detectors were trained using contrast adjustment based on highlighting the bone in the samples.

### C. Results and Discussion

Localization of the top of the iliac crest was tested in 60 CT volumes which contained the pelvis and succeeded in all 60 cases. The algorithm successfully determined no

pelvis was present in 8 of 10 additional cases consisting of chest and abdominal CT volumes which did not contain the pelvis. Localization of the top slice containing the liver was tested on 71 cases and was localized within 1 cm in 87% of volumes. Axial localization of the spleen succeeded in 40 of 42 test volumes.

Our algorithm performed with an average Dice score of 0.873 on 37 annotated cases. Spleen localization failed on two cases out of 39. We do not have access to data needed to compare our method to current models, such as contrast phase information. Furthermore, most previous work focuses on multi-organ segmentation rather than just spleen segmentation and the authors are able to improve their results via multi-organ refinement steps. In addition, our datasets specifically contain patients with blunt chest, pelvic, and abdominal injuries, the presence of which introduces further obstructions to segmentation in terms of additional variation in size and shape as well as presence of other artifacts in the abdomen such as hemotoma and blood. The robustness of published methods in the presence of these various traumas is unclear.

Localization was performed on an additional two volumes for which expert annotation was unavailable due to the severity of spleen lacerations present in the volumes. Figure 4 shows segmentation results on three separate patients with spleen lacerations. The left and center subjects' injuries were too severe for annotation to be provided. The patient on the right's lacerated spleen was segmented with a Dice score of 0.937.

### IV. CONCLUSION AND FUTURE WORK

Automated spleen segmentation can help fast diagnosis of splenic injury. Here, we proposed a fully automated spleen localization method followed by segmentation. It requires only a very rough, small-pixel-region localization of the spleen in order to provide segmentation via active contours. The spleen was segmented with an average Dice score of 0.873 and a highest Dice score of 0.938. Advantages include that method does not require image registration or use of any atlas-based methods. Future work will focus on creating a 2-D segmentation refinement step and obtaining more ground truth segmentations for testing. Ultimately, our goal is to incorporate spleen segmentation in a CAD system for long-term spleen monitoring and detection of blunt splenic injury.

# ACKNOWLEDGMENT

This material is based upon work supported by the National Science Foundation under Grant No. 1500124.

### REFERENCES

- [1] Radhiana Hassan, Azian Abd Aziz, Ahmad Razali Md Ralib, and Azlin Saat. Computed Tomography of Blunt Spleen Injury: A Pictorial Review. *The Malaysian journal of medical sciences: MJMS*, 18(1):60–67, 2011.
- [2] Jessica R. Leschied, Michael B. Mazza, Matthew S. Davenport, Suzanne T. Chong, Ethan A. Smith, Carrie N. Hoff, Maria F. Ladino-Torres, Shokoufeh Khalatbari, Peter F. Ehrlich, and Jonathan R. Dillman. Inter-radiologist agreement for CT scoring of pediatric splenic injuries and effect on an established clinical practice guideline. Pediatric Radiology, 46(2):229–236, February 2016. 00003.







Fig. 4: Segmentation results on lacerated spleens.

- [3] P. Prassopoulos, M. Daskalogiannaki, M. Raissaki, A. Hatjidakis, and N. Gourtsoyiannis. Determination of normal splenic volume on computed tomography in relation to age, gender and body habitus. *European Radiology*, 7(2):246–248, March 1997.
- [4] Alexandre S. Bezerra, Giuseppe D'Ippolito, Salomo Faintuch, Jacob Szejnfeld, and Muneeb Ahmed. Determination of Splenomegaly by CT: Is There a Place for a Single Measurement? *American Journal of Roentgenology*, 184(5):1510–1513, May 2005.
- [5] Peijun Hu, Fa Wu, Jialin Peng, Yuanyuan Bao, Feng Chen, and Dexing Kong. Automatic abdominal multi-organ segmentation using deep convolutional neural network and time-implicit level sets. *International* journal of computer assisted radiology and surgery, 12(3):399–411, 2017.
- [6] Xiangrong Zhou, Song Wang, Huayue Chen, Takeshi Hara, Ryujiro Yokoyama, Masayuki Kanematsu, and Hiroshi Fujita. Automatic localization of solid organs on 3d CT images by a collaborative majority voting decision based on ensemble learning. Computerized Medical Imaging and Graphics, 36(4):304–313, June 2012.
- [7] Marius George Linguraru, Jesse K. Sandberg, Zhixi Li, Furhawn Shah, and Ronald M. Summers. Automated segmentation and quantification of liver and spleen from CT images using normalized probabilistic atlases and enhancement estimation. *Medical Physics*, 37(2):771–783, February 2010.
- [8] Tong Tong, Robin Wolz, Zehan Wang, Qinquan Gao, Kazunari Misawa, Michitaka Fujiwara, Kensaku Mori, Joseph V. Hajnal, and Daniel Rueckert. Discriminative dictionary learning for abdominal multiorgan segmentation. *Medical Image Analysis*, 23(1):92–104, 2015.
- [9] Toshiyuki Okada, Marius George Linguraru, Masatoshi Hori, Ronald M. Summers, Noriyuki Tomiyama, and Yoshinobu Sato. Abdominal multi-organ segmentation from CT images using conditional shape-location and unsupervised intensity priors. *Medical Image Analysis*, 26(1):1–18, December 2015.
- [10] Baochun He, C Huang, and Fucang Jia. Fully automatic multi-organ segmentation based on multi-boost learning and statistical shape model search. CEUR Workshop Proceedings, 1390:18–21, January 2015.
- [11] P. Campadelli, E. Casiraghi, and S. Pratissoli. Fully automatic segmentation of abdominal organs from ct images using fast marching methods. In 2008 21st IEEE International Symposium on Computer-Based Medical Systems, pages 554–559, June 2008.
- [12] Jiaqi Liu, Yuankai Huo, Zhoubing Xu, Albert Assad, Richard G. Abramson, and Bennett A. Landman. Multi-atlas spleen segmentation on CT using adaptive context learning. volume 10133, pages 1013309– 1013309–7, 2017.
- [13] Zhoubing Xu, Bo Li, Swetasudha Panda, Andrew J. Asman, Kristen L. Merkle, Peter L. Shanahan, Richard G. Abramson, and Bennett A. Landman. Shape-Constrained Multi-Atlas Segmentation of Spleen in CT. Proceedings of SPIE-the International Society for Optical Engineering, 9034:903446, March 2014.
- [14] S. M. Reza Soroushmehr, Pavani Davuluri, Somayeh Molaei, Rosalyn Hobson Hargraves, Yang Tang, Charles H. Cockrell, Kevin Ward, and Kayvan Najarian. Spleen Segmentation and Assessment in CT Images for Traumatic Abdominal Injuries. *Journal of Medical Systems*, 39(9):87, September 2015. 00001.
- [15] P. Viola and M. Jones. Rapid object detection using a boosted cascade of simple features. In *Proceedings of the 2001 IEEE Computer Society Conference on Computer Vision and Pattern Recognition. CVPR 2001*, volume 1, pages I–511–I–518 vol.1, 2001.
- [16] T. F. Chan and L. A. Vese. Active contours without edges. *IEEE Transactions on Image Processing*, 10(2):266–277, February 2001.